Journal of Magnetic Resonance 208 (2011) 27–33

Contents lists available at ScienceDirect

Journal of Magnetic Resonance

journal homepage: www.elsevier.com/locate/jmr

A portable Halbach magnet that can be opened and closed without force: The NMR-CUFF

Carel W. Windt [a,b,*], Helmut Soltner [b,c], Dagmar van Dusschoten [a], Peter Blümler [a,b,1]

[a] ICG-3: Phytosphere, Forschungszentrum Jülich GmbH, 52425 Jülich, Germany
[b] Virtual Institute for Portable NMR (VIP-NMR), Forschungszentrum Jülich GmbH, 52425 Jülich, Germany
[c] ZAT: Central Technology Division, Forschungszentrum Jülich GmbH, 52425 Jülich, Germany

ARTICLE INFO

Article history:
Received 24 June 2010
Revised 23 September 2010
29 September 2010
Available online 30 October 2010

Keywords:
Permanent magnet
Halbach
Magic ring
Plants
Growth
Xylem flow
Long-distance transport

ABSTRACT

Portable equipment for nuclear magnetic resonance (NMR) is becoming increasingly attractive for use in a variety of applications. One of the main scientific challenges in making NMR portable is the design of light-weight magnets that possess a strong and homogeneous field. Existing NMR magnets can provide such magnetic fields, but only for small samples or in small regions, or are rather heavy. Here we show a simple yet elegant concept for a Halbach-type permanent magnet ring, which can be opened and closed with minimal mechanical force. An analytical solution for an ideal Halbach magnet shows that the magnetic forces cancel if the structure is opened at an angle of 35.3° relative to its poles. A first prototype weighed only 3.1 kg, and provided a flux density of 0.57 T with a homogeneity better than 200 ppm over a spherical volume of 5 mm in diameter without shimming. The force needed to close it was found to be about 20 N. As a demonstration, intact plants were imaged and water (xylem) flow measured. Magnets of this type (NMR-CUFF = Cut-open, Uniform, Force Free) are ideal for portable use and are eminently suited to investigate small or slender objects that are part of a larger or immobile whole, such as branches on a tree, growing fruit on a plant, or non-metallic tubing in industrial installations. This new concept in permanent-magnet design enables the construction of openable, yet strong and homogeneous magnets, which aside from use in NMR or MRI could also be of interest for applications in accelerators, motors, or magnetic bearings.

1. Introduction

Inexpensive, light-weight and versatile instruments are always welcome, in everyday life as much as in practical research. Portable NMR promises to provide such instruments, and can be expected to be of great advantage when measuring objects that are too large or too sensitive to be moved into the laboratory (e.g. plants, trees, walls, historical artifacts, or works of art) [1]. For NMR to become light-weight and portable, most parts of the spectrometer will have to be scaled down and reduced to the most indispensable parts. Scaling down the magnet here is one of the biggest challenges, and has already triggered several extremely innovative research activities and hardware developments [1,2]. However, in many applications the problem of portability cannot be solved by only making the magnet smaller. Immobile objects tend to be large, and if such an object is to fit inside it, the bore of the magnet should be larger still.

An elegant solution to get around this problem is provided by unilateral NMR. Here, when using a unilateral magnet such as for instance the NMR-MOUSE [3–5], the object does not have to fit inside the magnet at all. Instead, the magnet can simply be placed on the sample's surface, allowing the investigation of small regions close to the surface of arbitrarily large objects. However, this concept suffers from a low signal-to-noise ratio and an unavoidable strong magnetic field gradient normal to the magnet's surface, which can only be compensated in small regions. Data from larger volumes thus can only be obtained in a scanning approach and up to a limited depth, and are difficult to quantify. In unilateral NMR the strong gradient normal to the magnet's surface might be compensated by surrounding the object with more magnets, but this of course would limit the accessibility of the magnet.

Alternative solutions are available when a subject as a whole is large, but possesses parts that are comparatively small or slender, such that a magnet might fit around or over it. Such an object might, for example, be the branch of a tree, a growing fruit on a plant, or a non-metallic tube in an industrial- or experimental set-up. One of the most convenient permanent magnet types to use in this fashion is the classical C-shape magnet with a yoke [6–8]. Because of the C-shape the centre of the magnet is freely accessible: the magnet can simply be slid into place around an object of

* Corresponding author. Address: Forschungszentrum Jülich, ICG-3: Phytosphere, Geb. 06.2, Leo Brandt Street 1, 52425 Jülich, Germany. Fax: +49 (0)2461 612492.
E-mail address: c.windt@fz-juelich.de (C.W. Windt).
[1] Present address: Dept. of Physics, University of Mainz, Staudingerweg 7, 55099 Mainz, Germany.

1090-7807/$ - see front matter © 2010 Elsevier Inc. All rights reserved.
doi:10.1016/j.jmr.2010.09.020

interest. Further, this type of magnet can provide an excellent homogeneity and field strength. However, its practical usefulness for portable NMR is severely limited by its weight. Especially when wider air gaps or high field strengths are required, the presence of a sizeable iron yoke will make C-shape magnets too heavy to handle by hand.

A second homogeneous, enclosing type of permanent magnet that is frequently used in portable NMR is the Halbach magnet [9–11]. This type of magnet has a number of properties that make it very well suited for portable NMR. The Halbach layout (see Fig. 1) has been proven to yield the highest possible field per mass of used permanent-magnet material, while at the same time offering a good homogeneity over a large proportion of the bore [12]. Halbach magnets further have a very small stray field, making them easy and safe to handle; and possess a transverse B_0 field, which makes it possible to fit them with inexpensive, but highly effective solenoidal rf-coils. However, a serious drawback for practical portable use is the fact that Halbach magnets are shaped like a cylinder. As such, it is accessible only for objects that happen to fit the magnets' bore, that can be moved into the magnet, or that the magnet can be fitted over- or on top of. The limited accessibility of the classical Halbach layout will thus, in many cases, seriously hinder the practical application of the type of magnet in portable NMR.

In this paper we present a solution to this accessibility problem, in the shape of a simple, yet elegant concept for a Halbach-type permanent magnet that can be opened from the side without significant force, and closed around an object of interest: the NMR-CUFF (for Cut open, Uniform, Force Free). Because an ideal Halbach (dipole) magnet comprises all possible orientations of in-plane polarization vectors within its structure (see Fig. 1), there are not only attractive forces between the magnetic moments that make up the Halbach ring, but also repulsive ones. We postulate that there is an angle at which these forces cancel each other out and where the Halbach ring can be split and opened without force. We present an analytical solution to calculate that angle, and demonstrate and test its validity by constructing a prototype. We demonstrate the quality and practical usefulness of the NMR-CUFF in a number of applications, varying from NMR imaging and q-space flow mapping, to a simpler and more sensor-like application of the magnet in monitoring the growth of a poplar tree.

2. Theory

With modern rare-earth magnet materials impressive field strengths can be achieved. For instance, FeNdB magnets with a remanence B_r in excess of 1.3 T are readily available. A drawback of these powerful magnets is that, when two magnets are brought in close proximity of each other, the forces between them can be dangerously large. The attractive force F between two cubic magnets, which are placed on top of each other and are polarized in the same direction, with side length a and remanence B_r, can be approximated for short distances by *Maxwell*'s pulling force formula

$$F \approx \frac{B_r^2 a^2}{2\mu_0} \tag{1}$$

Here μ_0 denotes the permeability of free space [13]. For two small permanent magnets made of FeNdB, with a remanence of 1.3 T and side length of 1 cm, the force between the two magnets already approaches a substantial 60 N. When the side length is increased to 3 cm the attractive force even exceeds 500 N. To pull apart two such magnets would require considerably more force than can be exerted by hand. Considering the field strengths that are required in an NMR magnet, and the large magnets that are needed to achieve them, the construction of an openable magnet would thus, at first glance, appear to be an impossible proposition.

However, the forces between magnets show an angular dependence, which make it possible to choose an orientation for which the magnets show no force along their connecting line. This requirement already identifies the location where two halves of a Halbach magnet can be separated without force, because the force between pairs of magnets drops with the fourth power of their distance and thus only nearest neighbours need to be considered.

To approximate this angular position, the relevant equations were simplified by assuming an infinitely thin Halbach cylinder with a continuous in-plane distribution of dipoles to represent the magnets. The force on a dipole with magnetic moment $\vec{m}_1$ in the field $\vec{B}_2$ of another dipole is given by [14]:

$$\vec{F} = -\nabla(\vec{m}_1 \cdot \vec{B}_2) \tag{2}$$

The insertion of this dipole field gives:

$$\vec{F} = -\nabla\left[\frac{\mu_0}{4\pi}\left(3\frac{(\vec{m}_1 \cdot \vec{r})\cdot(\vec{m}_2 \cdot \vec{r})}{r^5} - \frac{(\vec{m}_1 \cdot \vec{m}_2)}{r^3}\right)\right] \tag{3}$$

where $\vec{r}$ is the connecting vector between the dipoles and r is the distance between them. The component of the force along the connecting vector for two parallel dipoles can be expressed in terms of the angle θ between their dipole moments and $\vec{r}$

$$F(\theta) = \frac{3\mu_0 m_1 m_2}{4\pi r^4}[3\cos^2\theta - 1] \tag{4}$$

The root $F(\theta_m) = P_2(\cos\theta_m) = 0$, of the second-order Legendre polynomial is the magic angle $\theta_m \approx 54{,}73°$, for which the force along the connecting line vanishes. This optimal angle coincides with the tangential vector $\vec{t} = (\cos\alpha, -\sin\alpha)$ to the shell, which in the yz coordinate system is perpendicular to the position vector $\vec{p} = (\sin\alpha, \cos\alpha)$ (Fig. 2).

The magnetization vector $\vec{m} = (\sin 2\alpha, \cos 2\alpha)$ however has twice the angle α relative to the z-axis at this position [15]. We therefore look for a position, where the angle between $\vec{t}$ and $\vec{m}$ equals θ_m, or

$$\begin{aligned} &\cos\theta_m = \vec{t}\cdot\vec{m} = \sin 2\alpha\cos\alpha - \sin\alpha\cos 2\alpha = \sin\alpha \\ &\text{or} \quad \alpha_m = \tfrac{\pi}{2} - \theta_m \approx 35.264° \end{aligned} \tag{5}$$

At this angular position (see Fig. 1) Halbach magnets can be split into two parts without attractive or repulsive forces along the connecting line. It should however be noted that in this

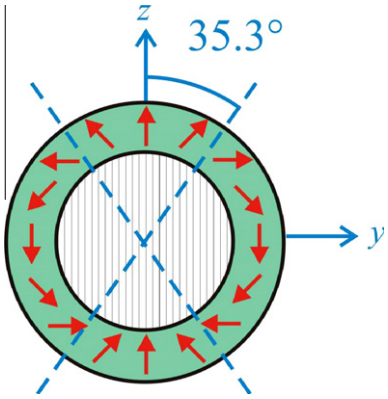

Fig. 1. Ideal Halbach dipole magnet ring: The permanent-magnet material is shown in green with its polarization direction specified by the red arrows. Such dipoles generate a strong and homogeneous magnetic field only inside the ring as indicated by the gray flux lines. The blue dashed lines indicate axes where the magnet can be opened without normal force. (For interpretation of the references to colour in this figure legend, the reader is referred to the web version of this article.)

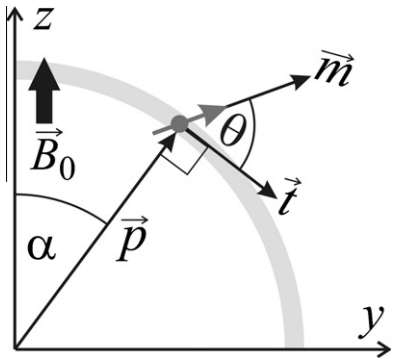

Fig. 2. Schematic illustration of the used geometry. The cross-section of a Halbach magnet (grey circle, only first quadrant shown) is represented by a shell of continuously distributed dipoles (dark grey dot with arrow). Each of these dipoles is characterized by its position $\vec{p}$ at an angle α, with the z-axis (which by convention defines the direction of the magnetic field B_0 of the Halbach magnet). The dipole moment has a direction vector $\vec{m}$, which forms an angle θ with the tangent $\vec{t}$ to the Halbach shell at this point.

configuration the shear forces are at their maximum. Fortunately the shear forces can easily be neutralized, for example by connecting the two magnet halves with hinges of sufficient strength.

3. Magnet design

The construction of permanent magnets for NMR has the inherent problem that, due to inaccuracies in the production process of the magnetic materials, the field strengths and magnetization angles of the magnet elements from which the final NMR magnets are constructed can vary considerably. From sample to sample their field strengths vary in the percent range, whereas the homogeneity of the assembled magnet should be at least one order of magnitude better. To circumvent this problem, a Halbach design has previously been proposed in which larger magnets are built from small but identical sub-pieces with known magnetic properties, the NMR-Mandhala [15–17]. This approach has the advantage that the homogeneity of the final magnet can be optimized by placing these individual sub-pieces at optimal positions, determined via analytical equations in a permutation algorithm.

For the first prototypes of an NMR-CUFF we chose to use only 4 magnets per ring (Fig. 3a), because such a design generates the highest field [15]. The magnet sub-pieces had dimensions of $30 \times 30 \times 10$ mm^3 and were made from grade 49 FeNdB, with a remanence of 1.42 T (Magnetic Components Engineering, Bedfordshire, UK). Of course this design does not allow to open the magnet at the optimal angle α_m, (see Fig. 3b), but 45° still is close enough to expect only small opening forces. For NMR-Mandhalas with more magnet elements a much better approximation of α_m can be achieved, for example with rings made from $n = 16$ identical magnets and split between the first and second magnet counted from the poles. For the $n = 4$ variant, with an opening angle of 45°, a boundary element method (BEM) simulation (Amperes, IES, Winnipeg, CA) was used to calculate the force needed to open the magnet. In this simulation the full geometry of the magnet assembly was taken into account, as well as the interactions of all magnets within it. The force was calculated to be about 57 N to split the assembly at the line of opening. In the NMR-CUFF, which is fitted with a hinge to neutralize the large shear forces in the plane of opening and to halve the force that is needed to open the magnet, this would result in an estimated opening force of 28.5 N. After building the magnet the force in fact proved to be even smaller than estimated, namely 20 N. The force thus was small enough to open and close the NMR-CUFF without effort.

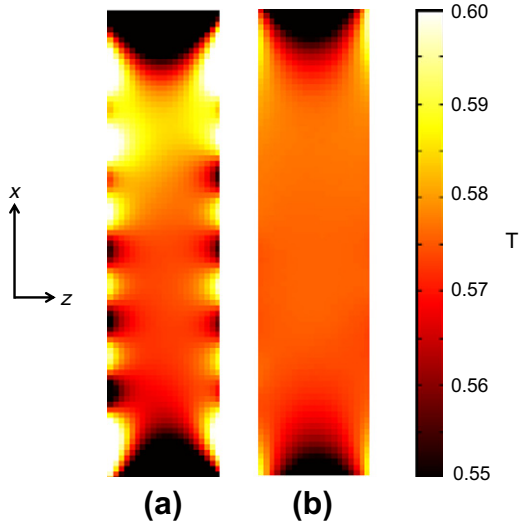

Fig. 4. Field homogenization by adding 1 mm steel polecaps. (a) NMR-CUFF without polecaps, (b) 1 mm thick polecaps mounted on the inner north- and south poles. Shown is a field plot along the xz-plane through the central cavity of an NMR-CUFF. Please note that in this demonstration polecaps were mounted on the inner poles only. In all other NMR-CUFFs in this study pole caps were placed on all poles of all four magnet stacks (i.e., eight polecaps in total). The magnetic field in the constructed magnet was scanned by means of a Hall-probe in combination with a home-built scanning robot, as previously described by Raich and Blümler [15].

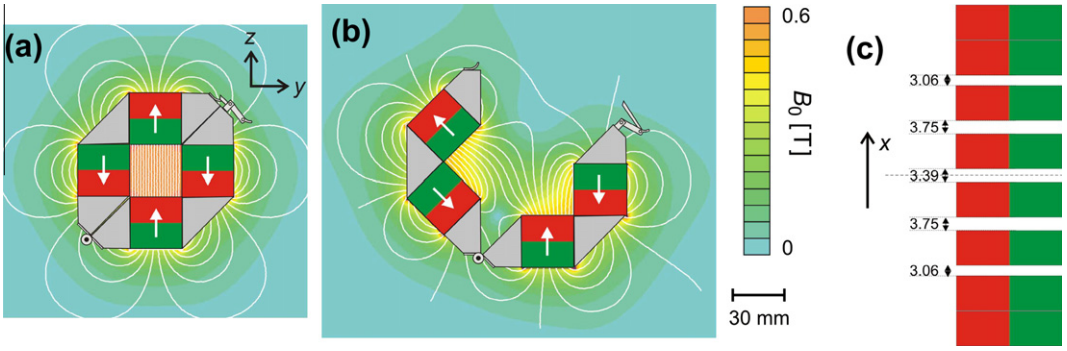

Fig. 3. Schematic representation of the used prototype: (a) The magnets have a size of 30 × 30 mm and enclose a sample space of the same size. The housing (grey) has a hinge at the lower left side and has a buckle at the opposite side. (b) Scheme showing the opened device. The colours in the background give the absolute flux density. The field lines are shown in white. (c) The magnets of height 1 cm are stacked in the third dimension, x, as shown. The five gaps are filled with precision machined aluminium spacers. The two magnets at the top of the stack, as well as the two magnets at the bottom, are stacked without any spacers in between. The arrangement is symmetric to the centre as indicated by the horizontal dashed line. The axes in (a) and (c) denote the coordinate system used in the text.

In principle the $n = 4$ Halbach variant presented here can be scaled up without difficulty. However, the opening force and the magnets weight may quickly become limiting factors. A doubling of the diameter of the magnets bore would be accompanied by an 8-fold increase in weight, if B_0 is to be kept constant [17], and the opening forces are expected to scale quadratically with the size of the magnet (e.g. see Eq. (1)). The opening force probably is the least problematic factor, as it can be reduced by choosing a Halbach variant that more closely matches the optimal opening angle. The increase in weight, however, will remain an important issue when scaling up the magnet. Other $n = 4$ Halbach implementations, such as the interesting design by Hills et al. [18] which has large spaces between the four magnet columns to allow for sideways access to the bore, could of course also be made to open from the side. Here, the wider apart the magnet columns are and the lower the resulting B_0 becomes, the easier it would be to open even large magnet assemblies.

To homogenize the field in the third dimension, the magnets were stacked with precision machined aluminium spacers in between (Fig. 3c). The optimal spacing of the magnets was iteratively determined by means of a second BEM simulation, following the methodology as described by Soltner and Blümler [17]. The stacks of magnet blocks and spacers were clamped together and fixed by means of aluminium top and bottom covers and a set of brass nuts and bolts. Finally the poles of each stack were covered by 1 mm thick iron sheets (i.e., pole caps) to further smooth the field (Fig. 4).

This prototype (see Fig. 5a) generates a flux density of 0.57 T in the closed configuration with a homogeneity better than 2×10^{-4} (200 ppm) over a spherical volume of 5 mm in diameter, a value that remained virtually unchanged even after repeated opening and closing of the magnet (Fig. 6). After shimming the magnetic field with a few iron platelets, $35 \times 10 \times 1.0\,\mathrm{mm}^3$ and $48 \times 10 \times 1.0\,\mathrm{mm}^3$ in size and placed in an iterative fashion on the outside of the NMR-CUFF, this value was improved to less than 50 ppm.

To allow 2D imaging and q-space flow measurements the system was equipped with two sets of plane-parallel gradient coils, one for the x and one for the z direction. Both were designed according to the winding path correction method as outlined by Vegh et al. [19]. In order to conserve space in the bore of the magnet a gradient in the y direction was omitted. There is however no fundamental reason why a y gradient might not be added. The first protoypes of a more tightly packed set of three dimensional

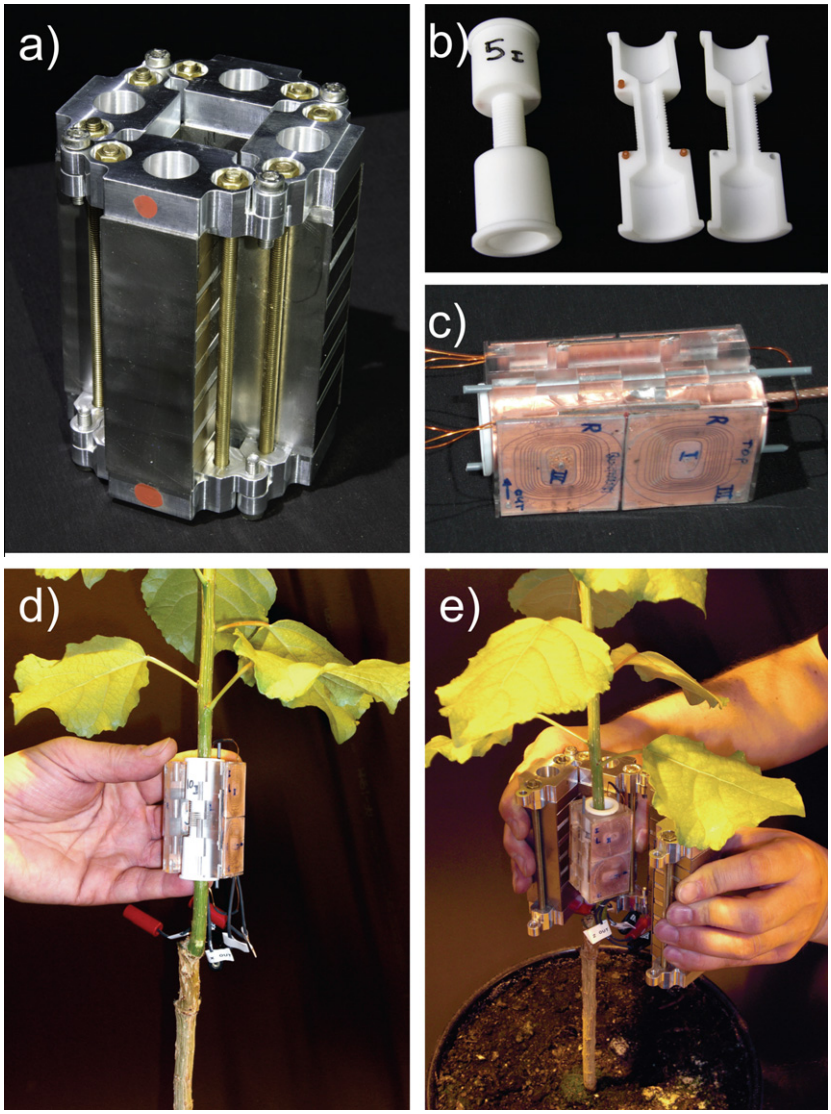

Fig. 5. Photographs of the final magnet system. (a) An NMR-CUFF prototype with four hinges or openings. (b) PTFE template for the solenoidal rf-coil. The rf-coil is hand wound on the threaded centre of the template. (c) The hinged, plane-parallel gradient system assembly, with an rf-coil inside. On the outside the x-gradient coils are visible. (d) Mounting the rf-coil and the gradient system on a plant stem and (e) finally enclosing it with the NMR-CUFF.

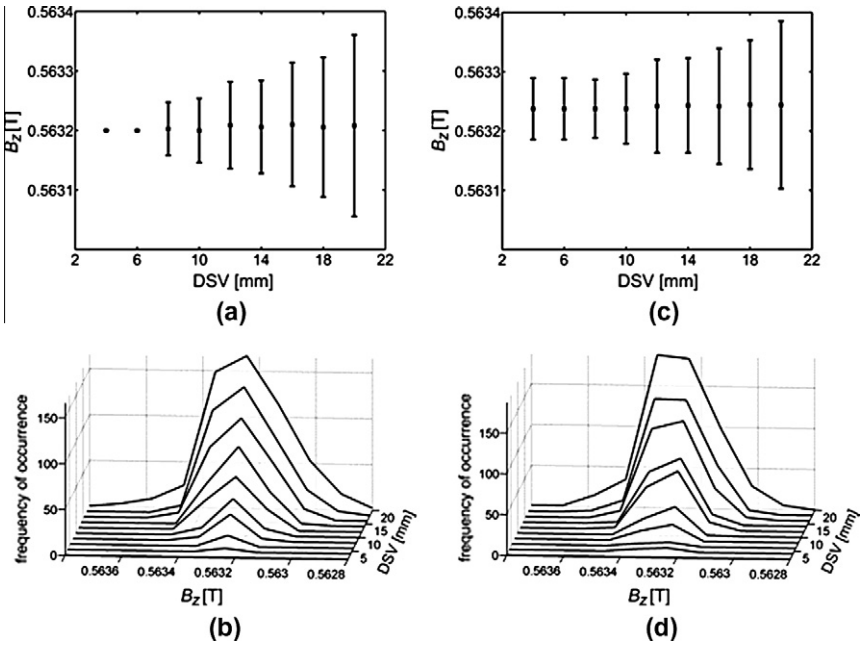

Fig. 6. Properties of the magnetic flux density for the NMR-CUFF in Fig. 5. On the left (a and b) measured direct after assembly, on the right (c and d) after opening and closing the magnet 10 times. (a and c) average flux density and standard deviation over a spherical volume of diameter DSV. (b and d) histograms of flux distribution. The flux density values were measured at 21 ± 1 °C using a scanning Hall-probe with an accuracy of 0.1 mT.

gradients have already been constructed (results not shown). The coils were laser-cut from 0.5 mm thick copper sheets. They produced gradients of 630 mT/m at 40 A and were mounted on the north- and south poles inside the magnet. The system was completed by a solenoidal rf-coil wound on a threaded PTFE template which can be split in half (see Fig. 5a and b) and tuned to resonate at the ^{1}H Larmor frequency (23.98 MHz).

4. Experimental

The NMR-CUFF was initially developed for applications in the plant sciences. Plants are prime examples of objects for which an NMR magnet, if the plant as a whole would need to fit inside it, would need to be huge, but where the object under study (a stem, or a fruit, etc.) typically is small. The NMR-CUFF can be expected to serve three main purposes in studying such objects: basic NMR imaging to study anatomy and dynamic changes therein; flow mapping to study water transport in the intact plant; and more sensor-like applications and basic relaxometry, for instance for on-line measurements of growth and water status. We here test and demonstrate the NMR-CUFF by means of three examples of such applications.

The magnet system was tested with three differently configured NMR spectrometers. Imaging was done using an NMR spectrometer consisting of a Resonance Instruments DRX console (Oxford Instruments, Abingdon, UK) equipped with a 500 W rf amplifier (Tomco, Norwood, Australia) and two BAFPA 40 gradient amplifiers (BRUKER, Rheinstetten, Germany). For the flow measurement a Bruker Avance spectrometer console was employed, equipped with a 500 W BLAX rf amplifier and a single BAFPA 40 gradient amplifier (BRUKER, Rheinstetten, Germany). For the third example a Kea 2 (Magritek, Wellington, New Zealand) spectrometer was used, equipped with a built-in 100 W rf amplifier.

First, in order to demonstrate the quality and imaging capability of the gradient system in combination with the NMR-CUFF, the non-invasive concept of the method was temporarily abandoned to allow for imaging the cross-section of a plant stem (Fig. 7a). As a demonstration object a ca. 3 mm thick piece of stem was excised from a 4-week-old castor bean (*Ricinus communis*) plant and inserted sideways into the NMR-CUFF, so that with the available gradients (x and z) a cross-section could be imaged. In the resulting (T_1 weighted) image the xylem tissue appears bright; the parenchyma in the centre appears darker. As already mentioned, there is no fundamental reason why it should not be possible to mount a third gradient as well; this would have made it possible to image the stem of a virtual slice in a living plant. However, in this setup we chose to conserve as much space as possible in the bore of the magnet by mounting only two sets of bi-planar gradients.

A second application of portable NMR in plants, and possibly the most interesting one, is measuring flow. The long-distance transport of water and nutrients inside the plant is of crucial importance for plant performance – in terms of yield, but also in terms of parameters such as water use efficiency, health, and product quality. This is illustrated by the fact that without it, plants would not be able to grow to sizes larger than a few centimeters. The two main transport pathways that take care of transport in the plant, the xylem and the phloem, have proven to be exceedingly difficult to study *in vivo*: both transport systems react with extreme sensitivity to any kind of conventional (i.e., invasive) plant physiological experimentation. NMR velocimetry, on the other hand, has been shown to be ideally suited to study these systems in the living plant. It has been applied to study transport in a variety of botanical subjects, such as seedlings, the main stem of plants and trees, and fruit stalks [20–24].

So far, quantitative q-space flow measurements in plants have only been done using full sized, stationary, high-end NMR instruments. Here, we demonstrate the first example of a xylem sap flow measurement done with a portable magnet on the stem of an intact plant (Fig. 7b). The magnet used here was the NMR-CUFF shown in Fig. 3. Coincidentally, this also constitutes the first example of a non-spatially resolved xylem flow measurement. So far the spatial resolution offered by MRI velocimetry has been used to separate the flow conducting from the non-flow conducting voxels. This procedure makes it possible to discard the voxels that do not contain flow, and lump together the voxels that do. This prevents the sometimes very small amounts of flowing water in

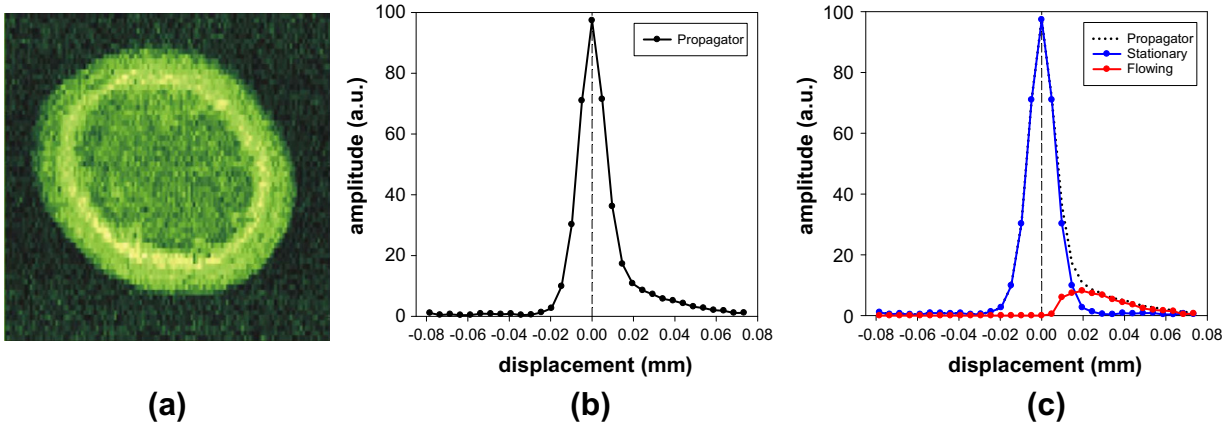

Fig. 7. Demonstrative NMR measurements with the NMR-CUFF: (a) NMR image of a 3 mm thick excised castor bean (*Ricinus communis*) stem slice with a diameter of 6 mm, acquired with a standard spin-echo sequence. Matrix size 64 × 128 pixels, field of view 7.5 × 7.5 mm^2. Repetition delay 0.5 s, 24 scans, scan time 26 min per image. A summation of 10 images is shown. (b) Flow measurement: propagator of water in the stem of an intact, 1.75 m tall poplar tree (*Populus nigra*, diameter ca. 7 mm). (c) Flow measurement: velocity spectra of stationary and flowing water. Xylem sap moving upward from roots to leaves is shown in red, stagnant water in tissues surrounding the vascular bundles is shown in blue. Experimental parameters: repetition time 2.5 s, echo time 3.5 ms, 32 echoes, eight averages, slice thickness 1.3 mm, spectral width 200 kHz. Scan time was about 11 min. The propagator was acquired by sampling q-space equidistantly, with gradient pulses from plus to minus 0.63 T/m in strength and 4 ms in duration, in combination with a labelling time of 20 ms.

the plant from being drowned out by the large amounts of stagnant water that typically also are present. Here, for lack of a y gradient, we did not have the possibility to follow the same methodology, but were nonetheless able to acquire a signal-to-noise ratio that was sufficient to separate the flowing from the stagnant water, and measure the xylem sap flow in a young poplar tree. The velocity spectrum of flowing water was obtained by mirroring the left half of the propagator (which gives the signal of the stationary but diffusing water and is assumed to be symmetrical to velocity = 0) at the ordinate and subtracting it from the right half of the propagator [25,26] (Fig. 7c).

A third example is the application of the NMR-CUFF in the role of a basic NMR-sensor. Since the emergence of genetically engineered crops, and the automated screening thereof, there has been an increasing demand for methods that allow parameters such as growth, water status and drought resistance to be measured in an on-line and non-invasive manner. These parameters could of course also be measured with conventional methods, but this typically would require the destruction of the plants in question. When only a few individuals of a certain genotype are in existence, this would be a highly undesirable course of action.

In this example we demonstrate the use of an NMR-CUFF to measure growth and water status in a young poplar tree. A potted poplar tree was grown in a climate chamber, with the NMR-CUFF mounted at the base of the trunk. In the climate chamber a 16 h light, 8 h dark cycle was applied, with a day temperature of 23 °C and a night temperature of 18 °C. Because of the relatively high temperature coefficient of the NdBFe magnet material that was employed in the NMR-CUFF, i.e., 0.11% B_r/K, the temperature of the magnet needed to be stabilized. For this reason the NMR-CUFF was fitted with a temperature controller based on two resistive heating foils, a PT100 based current controller and a power supply. In addition the magnet was covered with a 1 cm thick sheet of AF/Armaflex insulation foam (Armacell Enterprise GmbH, Münster, Germany). In this fashion the temperature of the magnet was kept constant at 30 ± 0.1 °C, irrespective of the changing ambient temperature and irradiation in the climate chamber.

In order to mimic an experiment that could be done using even the most basic of spectrometers, we chose to acquire a CPMG echo-train, but utilized only a single echo at 25 ms (experimental parameters: repetition time 2.5 s, echo time 150 μs, 32 averages, total scan time 80 s). The absolute value of the 16 points comprising this echo was taken, and the total amplitude used as a measure for the amount of liquid water in the stem of the tree. The experiment was subsequently allowed to run, fully automated, for a period of 3.5 days (Fig. 8). Despite the simplicity of the measurement the results turned out to be surprisingly accurate, with a variation of less than 1% for a similarly sized reference object. Diurnal changes in water status in the tree could easily be distinguished, and, surprisingly enough, even the growth of the tree trunk over the mere three and a half days that the experiment lasted, could clearly be discerned. The observed behaviour corresponds well with existing data in literature. The diameter of trees and plants will vary over the course of a day in response to changes in the negative pressures (suction) in the trees' xylem tissues, which occur as a result of differences in evaporation from the leaves. Over the course of the day strong negative pressures exist, causing shrinkage of the stem and sometimes even depleting storage pools of water that might be present there. At night the negative pressures disappear, and given that enough water is

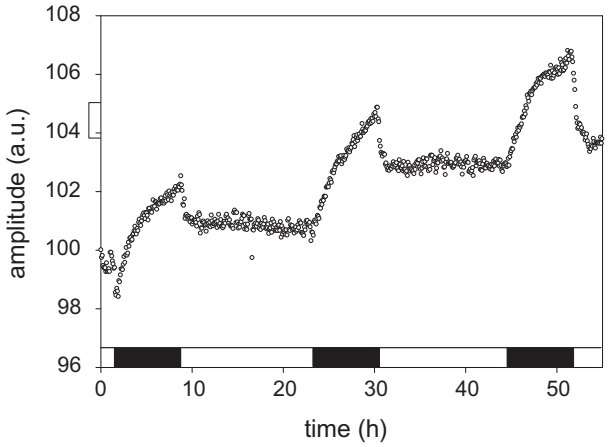

Fig. 8. The NMR-CUFF employed to measure changes in diurnal water status and growth in the trunk of a young poplar tree. A complete CPMG train was acquired (repetition time 2.5 s, echo time 150 μs, 32 averages, spectral width 250 kHz, 16 points per echo, total scan time 80 s), but only a single echo at TE = 25 ms was utilized. Every point represents the integral of the absolute values of the 16 points comprising this echo, normalized to $t = 0$. The bar in the bottom of the graph indicates day (white) and night (black).

available in the soil, the stem expands and storage pools are refilled [27].

5. Conclusion

By virtue of their small weight, high field strength and good homogeneity, hinged Halbach magnet systems of the NMR-CUFF design are ideally suited for samples which as a whole are too large to fit into a normal NMR magnet, but in which the section of interest is small or slender. Examples of such objects are non-metallic tubes in experimental or industrial setups, extremities and necks in animals or humans, or stems and branches in plants. Our prototype was tailor-made to investigate the latter and can be expected to open a new field in plant research by means of NMR-methods. The great potential of mobile NMR-equipment for use in the plant sciences has already been demonstrated [7,28]. However, the systems that have been introduced so far are too heavy to be used in the field routinely. Admittedly, such an operation also would require portable, backpack-sized spectrometers and amplifiers. Such spectrometers now slowly are becoming available. Furthermore, the magnet systems would require light-weight means of stabilization against varying temperature (e.g. by locking the NMR-frequency of a reference experiment) and additional field homogenization by shimming coils or small correcting permanent magnets [10,29,30]. Such advancements might also allow for spectroscopic NMR-methods [4,31]. The unexpectedly straightforward solution offered by hinged Halbach magnets, which makes them openable with virtually no force, is conceptually interesting also for non-NMR applications [32]. Wherever strong and homogeneous magnetic fields have to be applied to larger volumes with limited accessibility, for example for temporary tests or measurements, this concept may find new and effective applications.

Acknowledgments

The authors would like to thank N. Hermes, A. Dahmen and J. Kochs for help in the construction of the NMR-CUFF prototypes, and H. Glückler and H. Peerenboom for producing the laser-cut gradient coils. We thank H. Van As (Wageningen University, the Netherlands) for the use of equipment in his lab during testing. Prof. U. Schurr is gratefully acknowledged for enabling the presented research.

References

[1] B. Blümich, The incredible shrinking scanner, Sci. Am. November (2008) 68–73.
[2] B. Goodson, Mobilizing magnetic resonance, Phys. World May (2006) 28–33.
[3] B. Blümich, J. Perlo, F. Casanova, Mobile single-sided NMR, Prog. Nucl. Magn. Reson. Spectrosc. 52 (2008) 197–270.
[4] J. Perlo, V. Demas, F. Casanova, C.A. Meriles, J. Reimer, A. Pines, B. Blümich, High-resolution NMR spectroscopy with a portable single-sided sensor, Science 308 (2005) 1278.
[5] L. Paulsen, L.S. Bouchard, D. Graziani, B. Blümich, A. Pines, Volume-selective magnetic resonance imaging using an adjustable, Single-sided, portable sensor, Proc. Nat. Acad. Sci. USA 105 (2008) 20601–20604.
[6] S. Utsuzawa, K. Fukuda, D. Sakaue, Use of magnetic resonance microscopy for the nondestructive observation of xylem cavitation caused by pine wilt disease, Phytopathology 95 (2005) 737–743.
[7] M. Rokitta, E. Rommel, U. Zimmermann, A. Haase, Portable nuclear magnetic resonance imaging system, Rev. Sci. Instr. 71 (2000) 4257–4262.
[8] S.M. Wright, D.G. Brown, J.R. Porter, D.C. Spence, E. Esparza, D.C. Cole, F.R. Huson, A desktop magnetic resonance imaging system, Magn. Reson. Mat. Phys. Biol. Med. 13 (2002) 177–185.
[9] K. Halbach, Strong rare-earth cobalt quadrupoles, IEEE Trans. Nucl. Sci. NS-26 (1979) 3882–3884.
[10] E. Danieli, J. Mauler, J. Perlo, B. Blümich, F. Casanova, Mobile sensor for high-resolution NMR spectroscopy and imaging, J. Magn. Reson. 54 (2009) 80–87.
[11] K. Halbach, Design of permanent multipole magnets with oriented rare-earth cobalt material, Nucl. Inst. Meth. 169 (1980) 1–10.
[12] V.N. Samofalov, D.P. Belozorov, A.G. Ravlik, Optimization of systems of permanent magnets, Phys. Met. Metall. 102 (2006) 494–505.
[13] D.J. Griffiths, Introduction to Electrodynamics, Prentice Hall, Upper Saddle River, NJ, 1999.
[14] T.H. Boyer, The force on a magnetic dipole, Am. J. Phys. 56 (1988) 688–692.
[15] H. Raich, P. Blümler, Design and construction of a dipolar halbach array with a homogeneous field from N * 8 identical bar magnets -NMR-Mandhalas, Magn. Res. Eng. 23B (2004) 16–25.
[16] B.D. Armstrong, M.D. Lingwood, E.R. McCarney, E.R. Brown, P. Blumler, S. Han, Portable X-band system for solution state dynamic nuclear polarization, J. Magn. Reson. 191 (2008) 273–281.
[17] H. Soltner, P. Blümler, Dipolar Halbach magnet stacks made from identically shaped permanent magnets for magnetic resonance, Concept Magn. Reson. Part A 36A (2010) 211–222.
[18] B.P. Hills, K.M. Wright, D.G. Gillies, A low-field low-cost Halbach magnet array for open-access NMR, J. Mag. Reson. 175 (2005) 336–339.
[19] V. Vegh, H. Zhao, G.J. Galloway, D.M. Doddrell, I.M. Brereton, The design of planar gradient coils. Part I: a winding path correction method, Concept Magn. Reson. Part B: Magn. Reson. Eng. 27B (2005) 17–24.
[20] W. Köckenberger, J.M. Pope, Y. Xia, K.R. Jeffrey, E. Komor, P.T. Callaghan, A non-invasive measurement of phloem and xylem water flow in castor bean seedlings by nuclear magnetic resonance microimaging, Planta 201 (1997) 53–63.
[21] C.W. Windt, F.J. Vergeldt, P.A. de Jager, H. Van As, MRI of long-distance water transport: a comparison of the phloem and xylem flow characteristics and dynamics in poplar, castor bean, tomato and tobacco, Plant Cell Environ. 29 (2006) 1715–1729.
[22] C.W. Windt, E. Gerkema, H. Van As, Most water in the tomato truss is imported through the xylem, not the phloem: a nuclear magnetic resonance flow imaging study, Plant Physiol. 151 (2009) 830–842.
[23] N.M. Homan, C.W. Windt, F.J. Vergeldt, E. Gerkema, H. Van As, 0.7 and 3 T MRI and sap flow in intact trees: xylem and phloem in action, Appl. Magn. Reson. 32 (2007) 157–170.
[24] C.W. Windt, F.J. Vergeldt, H. Van As, Correlated displacement-T_2 MRI by means of a pulsed field gradient – multi spin echo method, J. Magn. Reson. 185 (2007) 230–239.
[25] T.W.J. Scheenen, D. van Dusschoten, P.A. de Jager, H. Van As, Microscopic displacement imaging with pulsed field gradient turbo spin-echo NMR, J. Magn. Reson. 142 (2000) 207–215.
[26] C.W. Windt, F.J. Vergeldt, P.A. De Jager, H. Van As, MRI of long-distance water transport: a comparison of the phloem and xylem flow characteristics and dynamics in poplar, Castor bean, tomato and tobacco, Plant Cell Environ. 29 (2006) 1715–1729.
[27] I. Offenthaler, P. Hietz, H. Richter, Wood diameter indicates diurnal and long-term patterns of xylem water potential in Norway spruce, Trees 15 (2001) 215–221.
[28] H. Van As, J.E.A. Reinders, P.A. Jager, P.A.C.M. van den Sanden, T.J. Schaafsma, In-situ plant water-balance studies using a portable NMR spectrometer, J. Exp. Bot. 45 (1994) 61–67.
[29] R.C. Jachmann, D.R. Trease, L.S. Bouchard, D. Sakellariou, R.W. Martin, R.D. Schlueter, T.F. Budinger, A. Pines, Multipole shimming of permanent magnets using harmonic corrector rings, Rev. Sci. Instr. 78 (2007) 0351151–0351157.
[30] J. Perlo, F. Casanova, B. Blümich, Ex situ NMR in highly homogeneous fields: H-1 spectroscopy, Science 315 (2007) 1110–1112.
[31] C.A. Meriles, D. Sakellariou, H. Heise, A.J. Moulé, A. Pines, Approach to high-resolution ex-situ NMR spectroscopy, Science 293 (2001) 82–85.
[32] J.M.D. Coey, Permanent magnet applications, J. Magn. Magn. Mat. 248 (2002) 441–456.